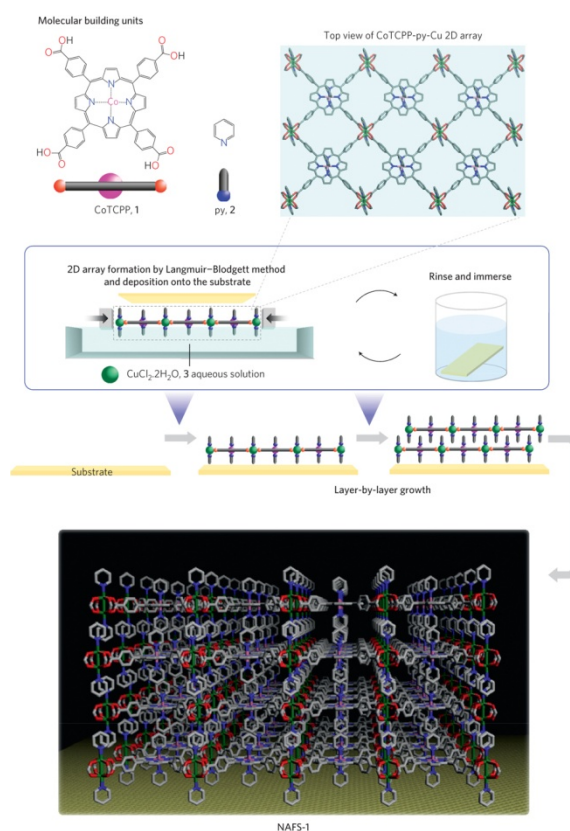


- Surface nano-architecture of a metal–organic framework

Makiura, R.; Motoyama, S.; Umemura, Y.; Yamanaka, H.; Sakata, O.; Kitagawa, H. *Nature Materials* **2010**, *9*, 565–571.

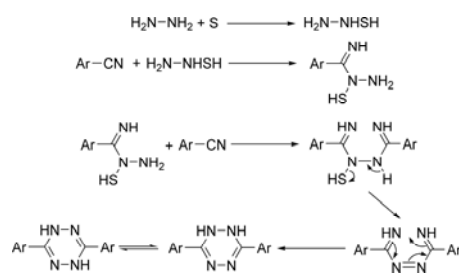
Abstract:



The rational assembly of ultrathin films of metal–organic frameworks (MOFs) - highly ordered microporous materials - with well-controlled growth direction and film thickness is a critical and as yet unrealized issue for enabling the use of MOFs in nanotechnological devices, such as sensors, catalysts and electrodes for fuel cells. Here we report the facile bottom-up fabrication at ambient temperature of such a perfect preferentially oriented MOF nanofilm on a solid surface (NAFS-1), consisting of metalloporphyrin building units. The construction of NAFS-1 was achieved by the unconventional integration in a modular fashion of a layer-by-layer growth technique coupled with the Langmuir–Blodgett method. NAFS-1 is endowed with highly crystalline order both in the out-of-plane and in-plane orientations to the substrate, as demonstrated by synchrotron X-ray surface crystallography. The proposed structural model incorporates metal-coordinated pyridine molecules projected from the two-dimensional sheets that allow each further layer to dock in a highly ordered interdigitated manner in the growth of NAFS-1. We expect that the versatility of the solution-based growth strategy presented here will allow the fabrication of various well-ordered MOF nanofilms, opening the way for their use in a range of important applications.

- s*-Tetrazines as Building Blocks for New Functional Molecules and Molecular Materials
Clavier, G.; Audebert, P. *Chem. Rev.* **2010**, *110*, 3299–3314.

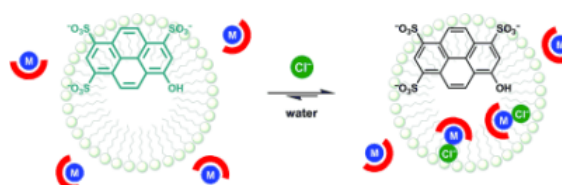
Abstract:



s-Tetrazines are long ago discovered molecules, whose first report dates back to the end of the 19th century. The first synthesis was reported by Pinner, who reacted equimolar quantities of hydrazine and benzonitrile and, after easy oxidation, isolated a red compound to which he assigned (rightfully by the way) the formula for 3,6-diphenyl-*s*-tetrazine from elemental analysis. Pinner prepared several other *s*-tetrazines in the same way, but did not go into many further investigations on their properties.

- A Micelle-Based Chemosensing Ensemble for the Fluorimetric Detection of Chloride in Water Riis-Johannessen, T.; Severin, K. *Chem. Eur. J.* **2010**, *16*, 8291-8295.

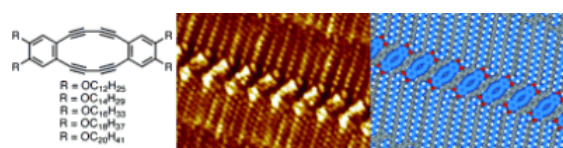
Abstract:



Caught in a trap! Fluorimetric chloride sensing in water is achieved by exploiting the changes in partition constant of a receptor complex in its bound and unbound states. In the presence of chloride, the complex preferentially resides in the micelle pseudo phase, where its contact with a fluorescent dye results in pronounced quenching effects (see figure).

- Self-Assembled Monolayers of Alkoxy-Substituted Octadecyhdibenzo[12]annulenes on a Graphite Surface: Attempts at *peri*-Benzopolyacene Formation by On-Surface Polymerization Tahara, K.; Inukai, K.; Hara, N.; Johnson II, C. A.; Haley, M. M.; Tobe, Y. *Chem. Eur. J.* **2010**, *16*, 8319-8328.

Abstract:



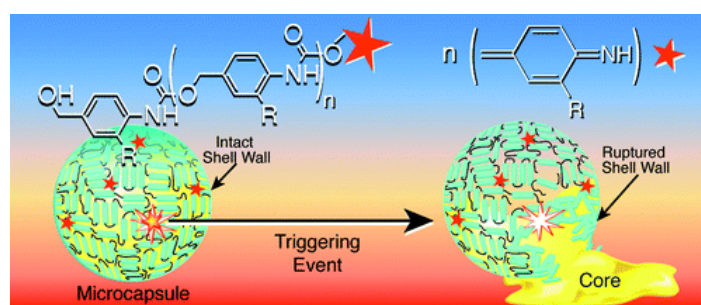
Self-assembled monolayers of a series of tetraalkoxy-substituted octadecyhdibenzo[12]annulene (DBA) derivatives **1 c-g** possessing butadiyne linkages were studied at the 1,2,4-trichlorobenzene (TCB) or 1-phenyloctane/graphite interface by scanning tunneling microscopy (STM). The purpose of this research is not only to investigate the structural variation of two-dimensional (2D) monolayers, but also to assess a possibility for *peri*-benzopolyacene formation by two-dimensionally controlled polymerization on a surface. As a result, the formation of three structures, porous, linear, and lamella structures, were observed by changing the alkyl chain length and the solute concentration. The formation of multilayers of the lamella structure was often observed for all compounds. The selection of molecular networks is basically ascribed to intermolecular and molecule-substrate interactions per unit area and network density. The selective appearance of the linear structure of **1 d** is attributed to favorable epitaxial registry matching between the substrate lattice and the

overlayer lattice. Even though the closest interatomic distance between the diacetylenic units of the DBAs in the lamella structure (≈ 0.6 nm) is slightly larger compared to the typical distances necessary for topochemical polymerization, the reactivity toward external stimuli (electronic-pulse irradiation from an STM tip and UV irradiation) was investigated. Unfortunately, no evidence for polymerization of the DBAs on the surface was observed. The present results indicate the necessity for further designing a suitable system for the on-surface construction of structurally novel conjugated polymers, which are otherwise difficult to prepare.

- Programmable Microcapsules from Self-Immolative Polymers

Esser-Kahn, A. P.; Sottos, N. R.; White, S. R.; Moore, J. S. *J. Am. Chem. Soc.* **2010**, *132*, 10266–10268.

Abstract:

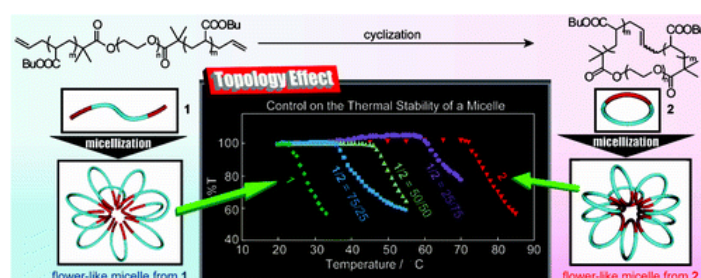


For the autonomous repair of damaged materials, microcapsules are needed that release their contents in response to a variety of physical and chemical phenomena, not just by direct mechanical rupture. Herein we report a general route to programmable microcapsules. This method creates core-shell microcapsules with polymeric shell walls composed of self-immolative polymer networks. The polymers in these networks undergo a head-to-tail depolymerization upon removal of the triggering end group, leading to breakdown of the shell wall and subsequent release of the capsule's liquid interior. We report microcapsules with shell walls bearing both Boc and Fmoc triggering groups. The capsules release their contents only under conditions known to remove these triggering groups; otherwise, they retain their contents under a variety of conditions. In support of the proposed release mechanism, the capsule shell walls were observed to undergo physical cracking upon exposure to the triggering conditions.

- Topology-Directed Control on Thermal Stability: Micelles Formed from Linear and Cyclized Amphiphilic Block Copolymers

Honda, S.; Yamamoto, T.; Tezuka, Y. *J. Am. Chem. Soc.* **2010**, *132*, 10251–10253.

Abstract:

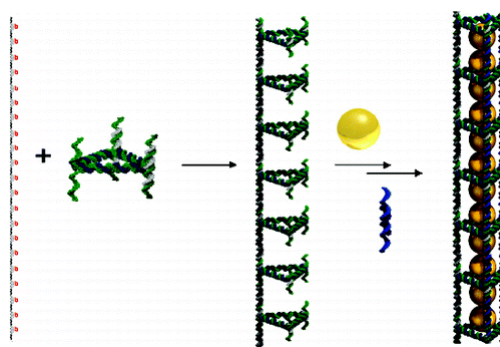


The thermal stability of a self-assembled micelle was remarkably enhanced by a topology effect. Linear poly(butyl acrylate)-*block*-poly(ethylene oxide)-*block*-poly(butyl acrylate) (**1**) and the cyclized product, poly(butyl acrylate)-*block*-poly(ethylene oxide) (**2**), were self-assembled to form flower-like

micelles. By means of viscometry, the critical micelle concentrations were determined to be 0.13 and 0.14 mg/mL for **1** and **2**, respectively. Dynamic light scattering, atomic force microscopy, and transmission electron microscopy studies revealed that both micelles are spherical and approximately 20 nm in diameter. Despite no distinctive change in the chemical composition or structure of the micelle, we found that the cloud point (T_c) was elevated by more than 40 °C through the linear-to-cyclic topological conversion of the polymer amphiphile. Furthermore, the T_c was tuned by coassembly of **1** and **2**.

- Templated Synthesis of DNA Nanotubes with Controlled, Predetermined Lengths
Lo, P. K.; Altvater, F.; Sleiman, H. F. *J. Am. Chem. Soc.* **2010**, *132*, 10212–10214.

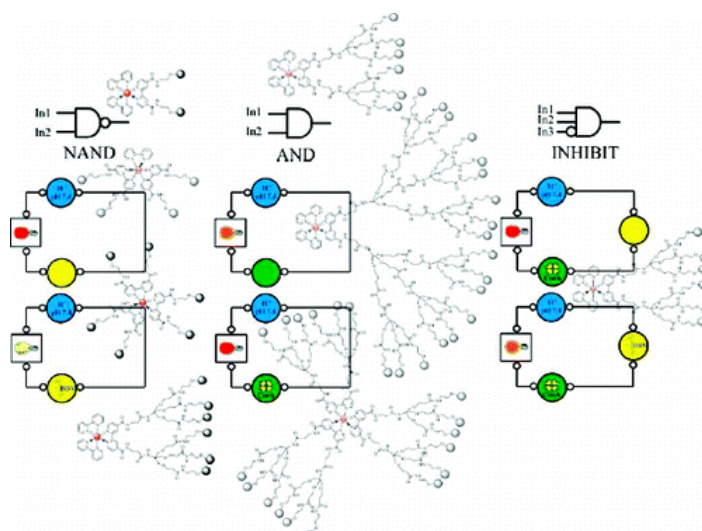
Abstract:



We report a DNA-templated approach to construct nanotubes with controlled lengths and narrow molecular weight distribution, allowing the deliberate variation of this length. This approach relies on the facile and modular assembly of a DNA guide strand of precise length that contains single-stranded gaps repeating at every 50 nm. This is followed by positioning triangular DNA “rungs” on each of these single-stranded gaps and adding identical linking strands to the two other sides of the triangles to close the DNA nanotubes. The length of the guide strand can be deliberately changed. We show the use of this approach to produce nanotubes with lengths of 1 μm or 500 nm and narrow length distributions. This is in contrast to nontemplated approaches, which lead to long and polydisperse nanotubes. We also demonstrate the encapsulation of 20 nm gold nanoparticles within these well-defined nanotubes to form finite lines of gold nanoparticles with longitudinal plasmon coupling, with a number of potential nanophotonic applications. This guiding strand approach is a useful tool in the creation of DNA nanostructures, in this case allowing the use of a simple template generated by a minimal number of DNA strands to program the length and molecular weight distribution of assemblies, as well as to organize any number of DNA-labeled nano-objects into finite structures.

- Lectin Biosensing Using Digital Analysis of Ru(II)-Glycodendrimers
Kikkeri, P.; Grünstein, D.; Seeberger, P. H. *J. Am. Chem. Soc.* **2010**, *132*, 10230–10232.

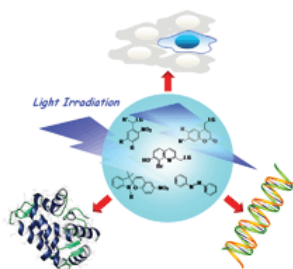
Abstract:



A novel, digital, single-operation analytical method to study glycodendrimer–lectin interactions is described. Robust, highly fluorescent derivatives of tris(bipyridine)ruthenium(II) ($[\text{Ru}(\text{bipy})_3]^{2+}$) bearing 2, 4, 6, or 18 mannose or galactose units were designed to perform molecular logic operations. Inputs for these systems were pH, N,N' -4,4'-bis(benzyl-2-boronic acid)bipyridinium dibromide, and different lectins (concanavalin A, Galantus nivalis agglutinin, and asialoglycoprotein). The relative change in fluorescence quantum yield of the Ru(II)-glycodendrimers served as output. Together, the fluorescent emission readout, the logic analysis of the photoinduced electron transfer, and the optical behavior provide a single-step method to quickly screen a glycodendrimer library and select the best dendrimer model for studying carbohydrate–lectin interactions.

- Photoactive molecules for applications in molecular imaging and cell biology
Shao, Q.; Xing, B. *Chem. Soc. Rev.* **2010**, *39*, 2835-2846.

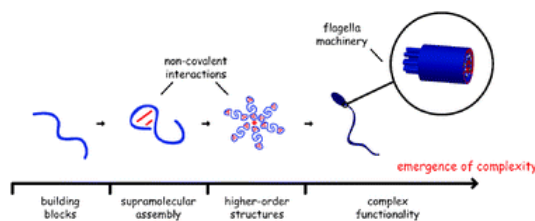
Abstract:



Photoactive technology has proven successful for non-invasive regulation of biological activities and processes in living cells. With the light-directed generation of biomaterials or signals, mechanisms in cell biology can be investigated at the molecular level with spatial and temporal resolution. In this *tutorial review*, we aim to introduce the important applications of photoactive molecules for elucidating cell biology on aspects of protein engineering, fluorescence labelling, gene regulation and cell physiological functions.

- Chemical complexity-supramolecular self-assembly of synthetic and biological building blocks in water
Zayed, J. M.; Nouvel, N.; Rauwald, U.; Scherman, O. A. *Chem. Soc. Rev.* **2010**, *39*, 2806-2816.

Abstract:

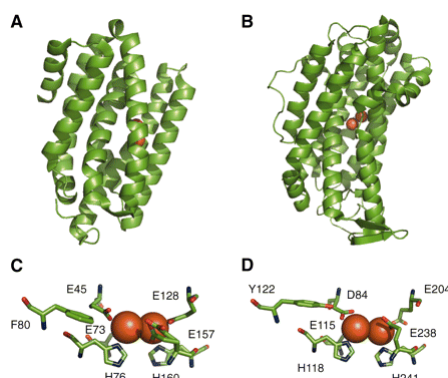


Aqueous supramolecular chemistry, the non-covalent assembly of simple building blocks into higher ordered architectures in water has received much focus recently. Biological systems are able to form complex, and well-defined microstructures essential to cellular function, and supramolecular chemistry has demonstrated its utility in assembling molecules to form increasingly complex assemblies. This *tutorial review* will summarise non-covalent building blocks based on both synthetic and biological systems in an aqueous environment, emphasising the complexity of the assemblies formed. Examples of higher ordered assemblies will be highlighted, from supramolecular plastics to spider silks, towards more compartmentalised *protocell* precursors.

- Microbial Biosynthesis of Alkanes

Schirmer, A.; Rude, M. A.; Li, X.; Popova, E.; del Cardayre, S. B. *Science* **2010**, *329*, 559 – 562.

Abstract:

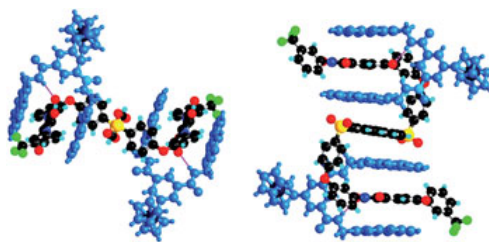


Alkanes, the major constituents of gasoline, diesel, and jet fuel, are naturally produced by diverse species; however, the genetics and biochemistry behind this biology have remained elusive. Here we describe the discovery of an alkane biosynthesis pathway from cyanobacteria. The pathway consists of an acyl–acyl carrier protein reductase and an aldehyde decarbonylase, which together convert intermediates of fatty acid metabolism to alkanes and alkenes. The aldehyde decarbonylase is related to the broadly functional nonheme diiron enzymes. Heterologous expression of the alkane operon in *Escherichia coli* leads to the production and secretion of C13 to C17 mixtures of alkanes and alkenes. These genes and enzymes can now be leveraged for the simple and direct conversion of renewable raw materials to fungible hydrocarbon fuels.

- Sequence-selective assembly of tweezer molecules on linear templates enables frameshift-reading of sequence information

Zhu, Z.; Cardin, C. J.; Gan, Y.; Colquhoun, H. M. *Nature Chemistry* **2010**, *2*, 653–660.

Abstract:

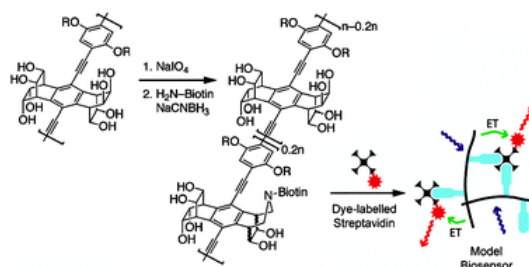


Information storage and processing is carried out at the level of individual macromolecules in biological systems, but there is no reason, in principle, why synthetic copolymers should not be used for the same purpose. Previous work has suggested that monomer sequence information in chain-folding synthetic copolyimides can be recognized by tweezer-type molecules binding to adjacent triplet sequences, and we show here that different tweezer molecules can show different sequence selectivities. This work, based on ^1H NMR spectroscopy in solution and on single-crystal X-ray analysis of tweezer–oligomer complexes in the solid state, provides the first clear-cut demonstration of polyimide chain-folding and adjacent-tweezer binding. It also reveals a new and entirely unexpected mechanism for sequence recognition, which, by analogy with a related process in biomolecular information processing, may be termed ‘frameshift-reading’. The ability of one particular tweezer molecule to detect, with exceptionally high sensitivity, long-range sequence information in chain-folding aromatic copolyimides is readily explained by this novel process.

- Biocompatible post-polymerization functionalization of a water soluble poly(p-phenylene ethynylene)

VanVeller, B.; Swager, T. M. *Chem. Commun.* **2010**, 46, 5761-5763.

Abstract:

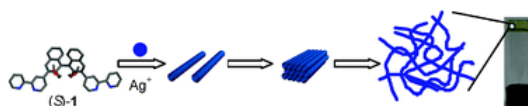


A biocompatible post-polymerization functionalization reaction takes advantage of a polymer's structural motif for the controllable attachment of biotin as a model biosensor that responds to streptavidin.

- Stereoselective and hierarchical self-assembly from nanotubular homochiral helical coordination polymers to supramolecular gels

He, Y.; Bian, Z.; Kang, C.; Gao, L. *Chem. Commun.* **2010**, 46, 5695-5697.

Abstract:

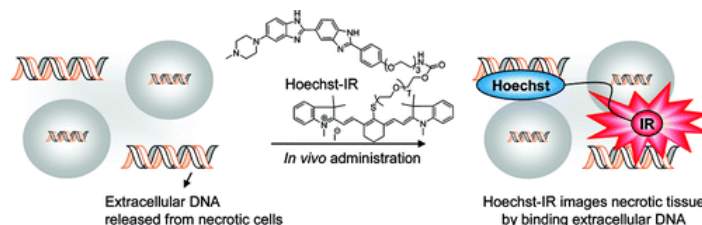


A new binaphthylbisbipyridine-based ligand underwent diastereoselective self-assembly with silver(I) ions to form nanotubular homochiral helical coordination polymers, which further hierarchically self-assemble into nanofibers, capable of immobilizing organic solvents.

- Hoechst-IR: An Imaging Agent That Detects Necrotic Tissue *In Vivo* by Binding Extracellular DNA

Dasari, M.; Lee, S.; Sy, J.; Kim, D.; Lee, S.; Brown, M.; Davis, M.; Murthy, N. *Org. Lett.* **2010**, *12*, 3300–3303.

Abstract :

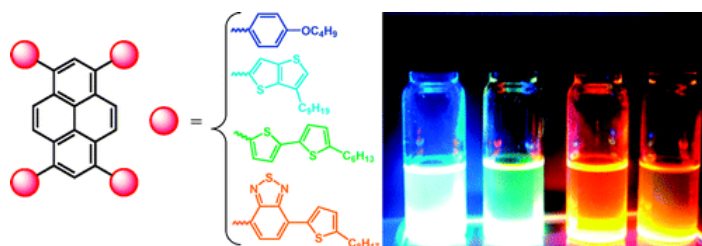


Cell necrosis is central to the progression of numerous diseases, and imaging agents that can detect necrotic tissue have great clinical potential. We demonstrate here that a small molecule, termed Hoechst-IR, composed of the DNA binding dye Hoechst and the near-infrared dye IR-786, can image necrotic tissue *in vivo* via fluorescence imaging. Hoechst-IR detects necrosis by binding extracellular DNA released from necrotic cells and was able to image necrosis generated from a myocardial infarction and lipopolysaccharide/D-galactosamine (LPS-GalN) induced sepsis.

- 1,3,6,8-Tetrasubstituted Pyrenes: Solution-Processable Materials for Application in Organic Electronics

Sonar, P.; Soh, M. S.; Cheng, Y. H.; Henssler, J. T.; Sellinger, A. *Org. Lett.* **2010**, *12*, 3292–3295.

Abstract:

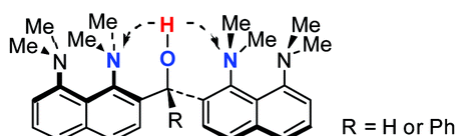


A series of star-shaped organic semiconductors have been synthesized from 1,3,6,8-tetrabromopyrene. The materials are soluble in common organic solvents allowing for solution processing of devices such as light-emitting diodes (OLEDs). One of the materials, 1,3,6,8-tetrakis(4-butoxyphenyl)pyrene, has been used as the active emitting layer in simple solution-processed OLEDs with deep blue emission (CIE = 0.15, 0.18) and maximum efficiencies and brightness levels of 2.56 cd/A and >5000 cd/m², respectively.

- 1,8,1',8'-Tetrakis(dimethylamino)-2,2'-dinaphthylmethanols: Double *In/Out* Proton Sponges with Low-Barrier Hydrogen-Bond Switching

Pozharskii, A. F.; Degtyarev, A. V.; Ozeryanskii, V. A.; Ryabtsova, O. V.; Starikova, Z. A.; Borodkin, G. S. *J. Org. Chem.* **2010**, *75*, 4706–4715.

Abstract:



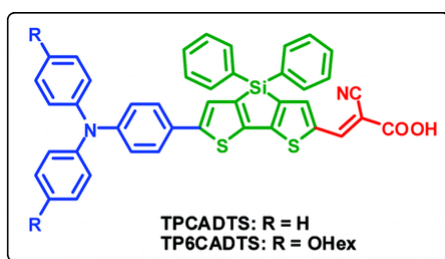
Rechelation or formation of O–H...O–H...N dimers depending on R, aggregate state, and temperature

Previously unknown bis[1,8-bis(dimethylamino)naphth-2-yl]phenylmethanol (**5**) and bis[1,8-bis(dimethylamino)naphth-2-yl]methanol (**6**) have been obtained and studied by combination of X-ray, NMR, and IR techniques at variable temperature. It has been established that both proton sponge units in the solid tertiary alcohol **5** exist in nonconventional *in/out* form, one of which is fixed by intramolecular O–H...N hydrogen bonding. In solution, a fast interconversion of two isoenergetic hydrogen chelates occurs which can be frozen below 183 K. Unlike this, the secondary alcohol **6** in the solid at 100 K adopts the *in/out-in/in* conformation and at 293 K demonstrates a kind of dynamic behavior which can be described as temperature-driven *dimer-induced rechelation*. In solution under ambient conditions **6** exists as an equilibrating mixture of chelated and unchelated monomeric forms in a ~1:1.8 molar ratio.

- Organic Dyes Containing Coplanar Diphenyl-Substituted Dithienosilole Core for Efficient Dye-Sensitized Solar Cells

Lin, L.-Y.; Tsai, C.-H.; Wong, K.-T.; Huang, T.-W.; Hsieh, L.; Liu, S.-H.; Lin, H.-W.; Wu, C.-C.; Chou, S.-H.; Chen, S.-H.; Tsai, A.-I. *J. Org. Chem.* **2010**, *75*, 4778–4785.

Abstract:



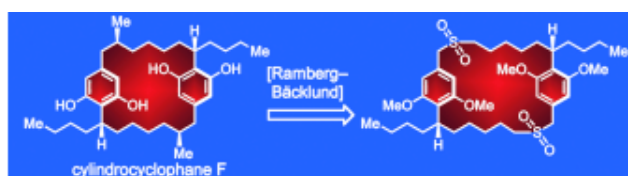
Under AM 1.5G, TP6CADTS-based DSSC gives an overall conversion efficiency of 7.60

Two new organic dyes adopting coplanar diphenyl-substituted dithienosilole as the central linkage have been synthesized, characterized, and used as the sensitizers for dye-sensitized solar cells (DSSCs). The best DSSC exhibited a high power conversion efficiency up to 7.6% (**TP6CADTS**) under AM 1.5G irradiation, reaching ~96% of the ruthenium dye **N719**-based reference cell under the same conditions.

- Asymmetric Total Synthesis of Cylindrocyclophanes A and F through Cyclodimerization and a Ramberg-Bäcklund Reaction

Nicolaou, K. C.; Sun, Y.-P.; Korman, H.; Sarlah, D. *Angew. Chem. Int. Ed.* **2010**, *49*, 5875-5878.

Abstract:



Two make a cycle: A Ramberg-Bäcklund reaction was employed to form the macrocyclic carbon skeleton of the marine natural products cylindrocyclophanes A and F in an asymmetric synthesis through a head-to-tail dimerization approach.

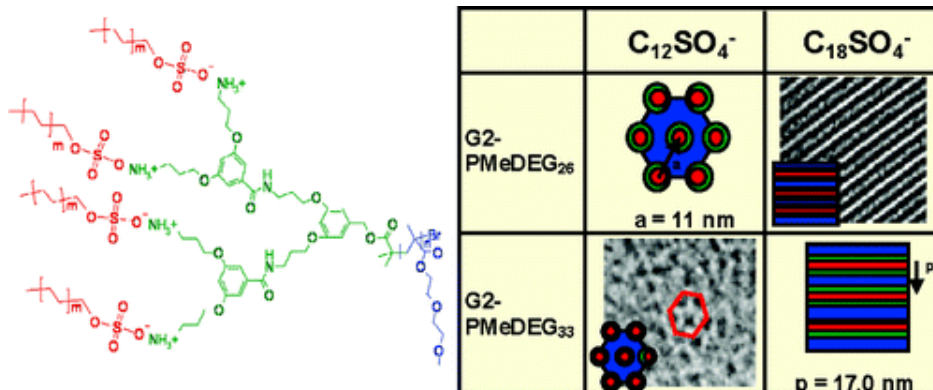
- Photochemical Addition of Ethers to C60: Synthesis of the Simplest [60]Fullerene/Crown Ether Conjugates

Tzirakis, M. D.; Orfanopoulos, M. *Angew. Chem. Int. Ed.* **2010**, *49*, 5891-5893.

Abstract:

Easy crowning for [60]fullerene: The simplest and hitherto elusive C60/crown ether conjugates have been prepared through an effective free-radical approach. This approach includes the activation of the otherwise unreactive -CH bond in a series of structurally diverse mono- or polyethers and sulfides. This facile method provides an expedient entry into a novel class of fullerene-based materials.

- Controlling Hierarchical Self-Assembly in Supramolecular Tailed-Dendron Systems
Merlet-Lacroix, N.; Rao, J.; Zhang, A.; Schlüter, D.; Bolisetty, S.; Ruokolainen, J.; Mezzenga, R.
Macromolecules **2010**, *43*, 4752–4760.

Abstract:

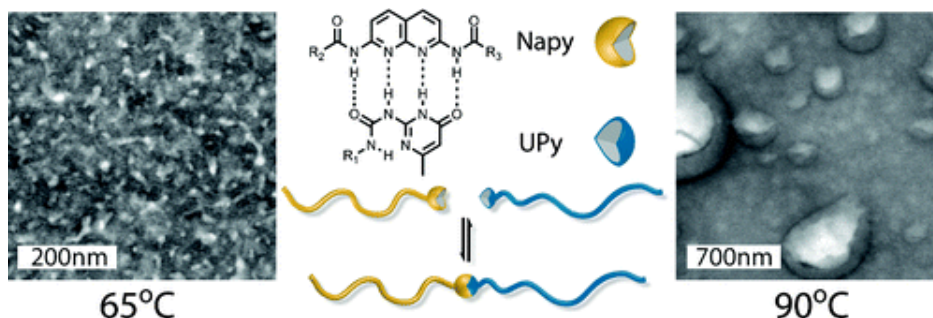
We study the self-assembly of a dendritic macromolecular system formed by a second-generation dendron with pH-responsive end groups and with a polymer chain emanating from its focal point, typically referred to as dendron-coil system. We use supramolecular ionic interactions to attach to the periphery of the dendrons sulfate-terminated alkyl tails of various lengths. The resulting ionic complexes have a molecular architecture similar to a four-arm dendritic pitchfork with varying arms and holder lengths. The bulk morphologies observed by small-angle X-ray scattering (SAXS) and transmission electron microscopy (TEM) show thermodynamically stable, hierarchical “inverted” hexagonal or lamellar structures. In addition, for a specific range of volume fractions, we show order-to-order transitions associated with the melting of the crystalline alkyl tails. The structural models for the molecular packing emerging from TEM and SAXS analysis are benchmarked to available self-consistent field theories (SCFTs) developed for identical systems and experiments and theoretical predictions are found in perfect agreement. With respect to our previous work on inverted dendron and dendrimer-surfactant self-assembled morphologies (Mezzenga et al. *Soft Matter*. **2009**, *5*, 92–97), the present findings show that keeping the same dendritic molecular architecture but adding a polymer chain emanating from the focal point enables the scale up of the structural organization

from the liquid crystalline length scale (10^0 nm) to the block copolymer length scale (10^1 nm) while preserving the inverted unconventional morphologies. Because the length of the holder and the arms of the dendritic pitchfork can be finely tuned, these systems offer new possibilities in the design of nanostructured organic materials and their use in templating applications.

- Phase Behavior of Complementary Multiply Hydrogen Bonded End-Functional Polymer Blends

Feldman, K. E.; Kade, M. J.; Meijer, E. W.; Hawker, C. J.; Kramer, E. J. *Macromolecules* **2010**, *43*, 5121–5127.

Abstract:



Blends of diamidonaphthyridine (Napy) end-functional poly(*n*-butyl acrylate) (PnBA) and ureidopyrimidinone (UPy) end-functional poly(benzyl methacrylate) (PbnMA) were studied as a function of the component molecular weights to compare with prior theoretical predictions. Macroscopic phase separation was observed to be prevented by the reversible association of end-functional polymers to form supramolecular diblock copolymers, resulting in stabilization of the interface between the polymers. At low molecular weights homogeneous microstructures were observed, in contrast to nonfunctional homopolymer blends of the same molecular lengths, which rapidly phase separate over macroscopic length scales. At higher molecular weights, the blend structure was reminiscent of compatibilized homopolymer blends, with the phase-separated domain size rapidly increasing with temperature. To compare with theoretical phase diagrams, the temperature-dependent Flory–Huggins χ parameter was measured, and it was found that PnBA/PbnMA covalent diblock copolymers show unusual lower critical ordering (LCOT) behavior with χ slightly increasing with temperature ($\chi(T) = 0.036 - 0.56/T$).